

systematic manner with the aid of frontier orbital theory and the Laplace concentration.

Acknowledgment. This research has been supported by a grant from the San Diego Supercomputer Center, which provided computer time at the CRAY-XMP/48. We thank Dr. Bowen Liu for helpful discussions. D.C. thanks the Deutsche For-

schungsgemeinschaft, the Fonds der Chemischen Industrie, and the Rechenzentrum der Universität Köln for support.

Registry No. He, 7440-59-7; Li⁺, 17341-24-1; Be⁺, 14701-08-7; B⁺, 14594-80-0; C⁺, 14067-05-1; N⁺, 14158-23-7; O⁺, 14581-93-2; F⁺, 14701-13-4; Ne⁺, 14782-23-1; BHe²⁺, 74891-40-0; CHE²⁺, 53262-54-7; HeN²⁺, 80896-02-2; HeO²⁺, 12269-22-6; HeF²⁺, 119455-36-6; HeNe²⁺, 57143-65-4.

Neon and Argon Bonding in First-Row Cations NeX⁺ and ArX⁺ (X = Li-Ne)¹

Gernot Frenking,*[†]

Molecular Research Institute, 701 Welch Road, Palo Alto, California 94304

Wolfram Koch,[‡]

Institut für Organische Chemie, Technische Universität Berlin, D-1000 Berlin 12, West Germany

Dieter Cremer,* Jürgen Gauss,

Institut für Organische Chemie, Universität Köln, Greinstrasse 4, D-5000 Köln 41, West Germany

and Joel F. Liebman*

Department of Chemistry, University of Maryland, Baltimore County Campus, Baltimore, Maryland 21228
(Received: August 19, 1988; In Final Form: November 7, 1988)

Theoretically determined equilibrium distances, vibrational frequencies, and dissociation energies for the first-row diatomic cations NeX⁺ and ArX⁺ (X = Li-Ne) in their ground and selected excited states are reported at the MP4(SDTQ)/6-311G(2df,2pd)//MP2/6-31G(d,p) level and compared with the results for HeX⁺. The dissociation energies D_e for the electronic ground states increase for a given X in the order HeX⁺ < NeX⁺ < ArX⁺, with the exception of X = Ne. The differences in D_e values between NeX⁺ and ArX⁺ are significantly larger than between HeX⁺ and NeX⁺. The binding energies for NeX⁺ and ArX⁺ show a distinct maximum for X = N. The trends in the calculated dissociation energies are rationalized by invoking donor-acceptor interactions between the weak electron donors Ne and Ar, respectively, and the electron acceptor X⁺. For this purpose, both frontier orbitals, electron density, energy density, and Laplace concentration are investigated. The analysis of the electronic structure shows that, in the case of the relatively weak acceptors Li⁺, Be⁺, and B⁺, the stability of the corresponding NeX⁺ and ArX⁺ ions in the ground state is solely due to charge-induced dipole interactions. Covalent bonding, however, is predicted for the ground state of NeN⁺, ArC⁺, ArN⁺, ArF⁺, and possibly NeNe⁺, as well as for most excited states of NeX⁺ and ArX⁺.

Introduction

In the preceding paper² (henceforth called I), we investigated the binding interactions in first-row cations HeX⁺. After having established a theoretical model for helium binding²⁻⁵ we now present an extension of our studies to neon and argon. We report our results of a "first-row sweep" of diatomic cations NeX⁺ and ArX⁺ (X = Li-Ne) and compare them with the data for the helium analogues HeX⁺. The aim of this study is to find out if the donor-acceptor model, which has been proven to be very helpful in explaining He chemistry,²⁻⁵ can also be used to rationalize the trends calculated for Ne and Ar compounds.

There are two major differences between He and the heavier analogues Ne and Ar. One is that, unlike helium, neon and argon have (filled) p orbitals in their valence shells. Therefore, π -orbital interactions with first-row elements Li-Ne in NgX⁺ (Ng = noble-gas element) are possible for Ng = Ne and Ar, but not He. A second difference is that the donor ability increases from He < Ne < Ar because the ionization energies (IE) become smaller (IE(He) = 24.587 eV, IE(Ne) = 21.564 eV, IE(Ar) = 15.759 eV).⁶ While the latter effect should yield stronger bonding for

Ar > Ne > He, the effect of π -orbital interactions will depend on the occupancy of the π orbitals of the binding partner X in NgX⁺. If X has occupied π orbitals, there will be additional π - π repulsion in NgX⁺ for Ng = Ne or Ar. If X has empty π orbitals, donor-acceptor interactions should be stronger. Our study will show that binding in most (but not all!) ground states of NgX⁺ (Ng = He, Ne, Ar) is caused largely by long-range forces with the dominant contribution at the equilibrium distance arising from charge-induced dipole interactions. It will be seen below that the

(1) Parts of this research have been reported in: (a) Frenking, G.; Koch, W. *Int. J. Mass Spectrom. Ion Processes* **1986**, *82*, 335. (b) Frenking, G.; Koch, W.; Deakynne, C.; Liebman, J. F.; Bartlett, N. J. *Am. Chem. Soc.* **1989**, *111*, 31.

(2) Frenking, G.; Koch, W.; Gauss, J.; Cremer, D.; Liebman, J. J. *J. Phys. Chem.*, preceding paper in this issue.

(3) Koch, W.; Frenking, G.; Gauss, J.; Cremer, D.; Collins, J. R. *J. Am. Chem. Soc.* **1987**, *109*, 5917.

(4) Frenking, G.; Koch, W.; Liebman, J. F. In *Molecular Structure and Energetics: Isoelectronic and Plemioelectronic Reasoning*; Liebman, J. F., Greenberg, A., Eds.; VCH Publishers: New York, 1989; p 1697.

(5) (a) Koch, W.; Collins, J.; Frenking, G. *Chem. Phys. Lett.* **1986**, *132*, 330. (b) Frenking, G.; Koch, W.; Gauss, J.; Cremer, D. *J. Am. Chem. Soc.* **1988**, *110*, 8007.

(6) Moore, C. E. *Analyses of Optical Spectra*; National Bureau of Standards; U.S. Government Printing Office: Washington, DC, 1970; NSRDS-NBS 34.

[†] Present address: Fachbereich Chemie, Universität Marburg, Hans-Meerwein-Strasse, D-3550 Marburg, West Germany.

[‡] Present address: IBM Wissenschaftliches Zentrum, Tiergartenstrasse 15, D-6900 Heidelberg, West Germany

TABLE I: Calculated Bond Lengths, r_e (Å), Total Energies, E_{tot} (hartrees), Vibrational Frequencies, ν (cm⁻¹), Zero-Point Vibrational Energies, ZPE, and Basis Set Superposition Errors, BSSE (kcal/mol), of NeX⁺ Ions.

| struct | sym | MP2/6-31G(d,p) | | | | MP4/6-311G(2df,2pd) | | |
|-------------------|--|----------------|------------------|-------|------------------|---------------------|------------------------|------|
| | | r_e | E_{tot} | ν | ZPE | r_e | E_{tot} | BSSE |
| NeLi ⁺ | X ¹ Σ ⁺ | 1.986 | -135.8758 | 272 | 0.4 | 2.032 | -136.0339 | 4.1 |
| NeBe ⁺ | X ² Σ ⁺ | 1.856 | -142.9140 | 259 | 0.4 | 2.054 | -143.0699 | 3.5 |
| NeB ⁺ | X ¹ Σ ⁺ | 2.474 | -152.9024 | 144 | 0.2 | 2.518 | -153.0808 | 1.6 |
| NeB ⁺ | ³ Π | 1.736 | -152.7684 | 380 | 0.5 | 1.736 | -152.9284 | 3.7 |
| NeC ⁺ | X ² Π | 2.077 | -165.9700 | 222 | 0.3 | | -166.1569 ^b | 1.9 |
| NeC ⁺ | ⁴ Σ ⁻ | 1.587 | -165.8306 | 601 | 0.9 | | -166.0002 ^b | 3.5 |
| NeN ⁺ | X ³ Σ ⁻ | 1.767 | -182.5768 | 393 | 0.6 | | -182.7806 ^b | 2.3 |
| NeO ⁺ | X ⁴ Σ ⁻ | 2.273 | -203.0377 | 198 | 0.3 | | -203.2653 ^b | 1.0 |
| NeO ⁺ | ² Π | 1.563 | -202.9125 | 661 | 0.9 | | -203.1539 ^b | 2.6 |
| NeF ⁺ | X ⁺ Π | 1.960 | -227.5076 | 266 | 0.4 | | -227.7725 ^b | 1.3 |
| NeF ⁺ | ¹ Σ ⁺ | 1.456 | -227.4593 | 876 | 1.3 | | -227.7375 ^b | 2.7 |
| NeNe ⁺ | X ² Σ ⁺ _g | 1.717 | -256.5374 | 571 | 0.8 ^a | | -256.8406 ^b | 1.7 |
| Li ⁺ | ¹ S | | -7.2359 | | | | -7.2358 | |
| Be ⁺ | ² S | | -14.2786 | | | | -14.2762 | |
| Be ⁺ | ² P | | -14.1319 | | | | -14.1298 | |
| B ⁺ | ¹ S | | -24.2715 | | | | -24.2896 | |
| B ⁺ | ³ P | | -24.1170 | | | | -24.1242 | |
| C ⁺ | ² P | | -37.3311 | | | | -37.3624 | |
| C ⁺ | ⁴ P | | -37.1640 | | | | -37.1733 | |
| N ⁺ | ³ P | | -53.9293 | | | | -53.9755 | |
| O ⁺ | ³ P | | -98.8712 | | | | -98.9780 | |
| Ne ⁺ | ² P | | -127.9494 | | | | -128.0037 | |
| Ne | ¹ S | | -128.6262 | | | | -128.7867 | |

^a Calculated at HF/6-31G(d,p). ^b At MP2/6-31G(d,p) optimized geometries.

calculated long-range interaction energies very often agree closely with the theoretically determined dissociation energies. However, the sometimes dramatic changes in the stabilities between ground states and some excited states of NgX⁺ and the sequence in the dissociation energies of NgX⁺ from Li to Ne finds a consistent explanation when the electronic structure of X is analyzed in terms of donor-acceptor interactions. The latter are described by investigating frontier orbitals, the electron density distribution $\rho(\mathbf{r})$, and its associated Laplace field.

Numerous investigations have been devoted to the interaction potentials of first-row atomic ions X⁺ and neon or argon, both experimentally and theoretically. However, only the theoretical papers of Liebman and Allen⁷ in the early 1970s addressed the question of comparing analogous NgX⁺ systems. Their studies were based on Hartree-Fock calculations and were restricted to only a few species of the complete set of NgX⁺ ions reported here. Other studies focused mostly on specific NgX⁺ molecules.

Perhaps the most extensively investigated systems are the lithium cations NeLi⁺ and ArLi⁺.⁸ SCF-CI calculations for ArLi⁺ in its ground state have been reported by Olson and Liu,^{8a} and the interaction potentials of NeLi⁺ and ArLi⁺ were the subject of several theoretical studies using the electron-gas model.^{8b-h} Scattering experiments^{8i-m} provide a very accurate knowledge of the Ne-Li⁺ and Ar-Li⁺ potentials. By contrast, the beryllium systems NeBe⁺ and ArBe⁺ are the least known cations of the NgX⁺ set. To our knowledge only NeBe⁺ has been the subject of a theoretical study⁹ without calculating the bond strength of

NeBe⁺. The binding energies of ArBe⁺ in the ground and excited states are known rather accurately from scattering experiments.¹⁰

NeB⁺ and ArB⁺ have recently been studied theoretically,^{11a} and a joint experimental/theoretical work on the potential interactions between boron ions and rare gases has been published by Ding, Hillier, Guest, and co-workers.^{11b} The same group also reported^{12a} theoretical and experimental results for ArC⁺. For the neon analogue NeC⁺ CASSCF results for the two lowest lying states have been published by us,^{12b} and the observation of NeC⁺ and ArC⁺ in the gas phase has recently been reported by Jonathan et al.^{12c} In the same study^{12c} the nitrogen and oxygen analogues NeN⁺, ArN⁺, NeO⁺, and ArO⁺ have been detected. Because the dissociation products were mainly Ng⁺ + X, it was concluded^{12c} that the NgX⁺ species were observed in their excited states. No data for the dissociation energies were given.

Scattering experiments for NeO⁺ and ArO⁺ and theoretical data for ArO⁺ are available from the studies of Ding, Guest, Hillier, and co-workers.¹³ The formation of ArF⁺ and the failure to observe NeF⁺ in gas-phase experiments were reported by Chupka and Berkowitz.^{14a} Scattering experiments and CASSCF calculations of NeF⁺ have very recently been published by Hottoka et al.^{14b} The noble-gas cations NeNe⁺ and NeAr⁺ were the subject of numerous theoretical^{15a-f} and experimental^{15g-j} investigations.

(7) (a) Liebman, J. F.; Allen, L. C. *J. Am. Chem. Soc.* **1970**, *92*, 3539. (b) Liebman, J. F.; Allen, L. C. *Int. J. Mass Spectrom. Ion Phys.* **1971**, *7*, 27. (c) Liebman, J. F.; Allen, L. C. *Inorg. Chem.* **1972**, *11*, 1143. (d) Liebman, J. F.; Allen, L. C. *J. Chem. Soc., Chem. Commun.* **1969**, 1355.

(8) (a) Olson, R. E.; Liu, B. *Chem. Phys. Lett.* **1979**, *62*, 242. (b) Gianturco, F. A. *J. Chem. Phys.* **1976**, *64*, 1973. (c) Gianturco, F. A.; Lamanna, U. T. *Physica B+C* **1978**, *93*, 279. (d) Waldman, M.; Gordon, R. G. *J. Chem. Phys.* **1979**, *71*, 1325. (e) Kim, Y. S.; Gordon, R. G. *J. Chem. Phys.* **1974**, *60*, 4323. (f) Kim, Y. S.; Gordon, R. G. *J. Chem. Phys.* **1974**, *61*, 1. (g) Gianturco, F. A.; Dilomardo, M. *J. Chim. Phys.* **1975**, *72*, 315. (h) Gianturco, F. A. *J. Chim. Phys.* **1976**, *73*, 527. (i) Wijnaendts van Resandt, R. W.; Champion, R. L.; Los, J. *Chem. Phys.* **1976**, *17*, 297. (j) Gatland, I. R. *J. Chem. Phys.* **1981**, *75*, 4162. (k) Polak-Dingels, P.; Rajan, M. S.; Gislason, E. A. *J. Chem. Phys.* **1982**, *77*, 3983. (l) Böttner; Dimpfl; Ross; Toennies *Chem. Phys. Lett.* **1975**, *32*, 197. (m) Viehland, L. A. *Chem. Phys.* **1983**, *78*, 279, and further references therein.

(9) Rzepa, H. S. *J. Mol. Struct. (THEOCHEM)* **1985**, *121*, 313.

(10) (a) Subbaram, K. V.; Coxon, J. A.; Jones, W. E. *Can. J. Phys.* **1976**, *54*, 1535. On the basis of the experimental data, slightly different dissociation energies have been predicted by: (b) Goble, J. H.; Hartman, D. C.; Winn, J. S. *J. Chem. Phys.* **1977**, *67*, 4206. (c) Goble, J. H.; Winn, J. S. *Chem. Phys. Lett.* **1981**, *77*, 168. (d) Goble, J. H.; Winn, J. S. *J. Chem. Phys.* **1979**, *70*, 2058. (e) Le Roy, R. J.; Lam, W.-H. *Chem. Phys. Lett.* **1980**, *71*, 544. (f) Vahala, L.; Havey, M. D. *J. Chem. Phys.* **1984**, *81*, 4867.

(11) (a) Iwata, S.; Sato, N. *J. Chem. Phys.* **1985**, *82*, 2346. (b) Ding, A.; Karlau, J.; Weise, J.; Kendrick, J.; Kuntz, P. J.; Hillier, I. H.; Guest, M. F. *J. Chem. Phys.* **1978**, *68*, 2206.

(12) (a) Hillier, I. H.; Guest, M. F.; Ding, A.; Karlau, J.; Weise, J. *J. Chem. Phys.* **1979**, *70*, 864. (b) Koch, W.; Frenking, G. *J. Chem. Phys.* **1987**, *86*, 5617. (c) Jonathan, P.; Boyd, R. K.; Brenton, A. G.; Beynon, J. H. *Chem. Phys.* **1986**, *110*, 239.

(13) (a) Guest, M. F.; Ding, A.; Karlau, J.; Weise, J.; Hillier, I. H. *Mol. Phys.* **1979**, *38*, 1427. (b) Ding, A.; Karlau, J.; Weise, J. *Chem. Phys. Lett.* **1977**, *45*, 92.

(14) (a) Berkowitz, J.; Chupka, W. *Chem. Phys. Lett.* **1970**, *7*, 447. (b) Hottoka, M.; Roos, B.; Delos, J. B.; Srivastava, R.; Sharma, R. B.; Koski, W. S. *Phys. Rev. A* **1987**, *35*, 4515.

CHART I: Dissociation Reactions of Ground and Excited States of NeX⁺ Cations: Calculated Dissociation Energies, D₀ and D_e, at MP4(SDTQ)/6-311G(2df,2pd)//MP2/6-31G(d,p) and Experimentally Derived D_e Data (kcal/mol)

| | this work | | other D _e | exptl D _e |
|--|-------------------|-------------------|--------------------------------------|--------------------------------------|
| | D _e | D ₀ | | |
| NeLi ⁺ (X ¹ Σ ⁺) → Ne(¹ S) + Li ⁺ (¹ S) | 3.0 | 2.6 | 2.8 ^k | 2.6 ^l |
| NeBe ⁺ (X ² Σ ⁺) → Ne(¹ S) + Be ⁺ (² S) | 0.9 | 0.5 | | |
| NeB ⁺ (X ¹ Σ ⁺) → Ne(¹ S) + B ⁺ (¹ S) | 1.2 | 1.0 | 3.7; ^g 0.5 ^l | |
| NeB ⁺ (³ Π) → Ne(¹ S) + B ⁺ (³ P) | 7.3 | 6.8 | 6.5; ^g 1.6 ^l | |
| NeC ⁺ (X ² Π) → Ne(¹ S) + C ⁺ (² P) | 3.0 | 2.7 | <0.2 ^l | |
| NeC ⁺ (⁴ Σ ⁻) → Ne(¹ S) + C ⁺ (⁴ P) | 21.7 | 20.8 | | |
| NeN ⁺ (X ⁴ Σ ⁻) → Ne(¹ S) + N ⁺ (³ P) | 9.2 | 8.6 | 2.3 ^d | |
| NeO ⁺ (X ⁴ Σ ⁻) → Ne(¹ S) + O ⁺ (⁴ S) | 1.2 | 0.9 | | |
| NeO ⁺ (² Π) → Ne(¹ S) + O ⁺ (² D) | 6.3 ^a | 5.4 ^a | | |
| NeF ⁺ (X ³ Π) → Ne(¹ S) + F ⁺ (³ P) | 3.6 | 3.2 | 0 ^h | |
| NeF ⁺ (¹ Σ ⁺) → Ne(¹ S) + F ⁺ (¹ D) | 39.8 ^b | 38.5 ^b | 30; ^e 37.9 ^h | |
| NeNe ⁺ (X ² Σ ⁺) → Ne(¹ S) + Ne ⁺ (² P) | 29.8 | 29.0 | 31.0; ^f 27.7 ^m | 30.0; ^c 31.1 ⁿ |

^a Calculated by using the atomic ground states and the experimentally derived³² excitation energy O⁺(⁴S) → O⁺(²D) (76.6 kcal/mol). ^b Calculated by using the atomic ground states and the experimentally derived³² excitation energy F⁺(³P) → F⁺(¹D) (59.6 kcal/mol). ^c Reference 18; ^d Reference 7b. ^e Reference 7a. ^f Reference 15d. ^g Reference 10a. ^h Reference 14b. ⁱ Reference 12b. ^j Reference 8k. ^k Reference 8d. ^l Reference 10b. ^m Reference 15a. ⁿ Reference 15h.

CHART II: Dissociation Reactions of Ground and Excited States of ArX⁺ Cations: Calculated Dissociation Energies, D₀ and D_e, at MP4(SDTQ)/6-311G(2df,2pd)//MP2/6-31G(d,p) and Experimentally Derived D_e Data (kcal/mol)

| | this work | | other D _e | exptl D _e |
|--|--------------------|--------------------|---|------------------------------------|
| | D _e | D ₀ | | |
| ArLi ⁺ (X ¹ Σ ⁺) → Ar(¹ S) + Li ⁺ (² S) | 5.7 | 5.3 | 6.2 ^k | 7.0; ^c 7.2 ^c |
| ArBe ⁺ (X ² Σ ⁺) → Ar(¹ S) + Be ⁺ (² S) | 10.9 | 10.4 | | 11.7 ^r |
| ArB ⁺ (X ¹ Σ ⁺) → Ar(¹ S) + B ⁺ (¹ S) | 5.6 | 5.4 | 8.1; ⁱ 2.1 ^j | 6.9 ^q |
| ArB ⁺ (³ Π) → Ar(¹ S) + B ⁺ (³ P) | 35.2 | 34.4 | 38.5; ⁱ 27.7 ^j | 34.6 ^r |
| ArC ⁺ (X ² Π) → Ar(¹ S) + C ⁺ (² P) | 20.6 | 20.2 | 27.2 ^l | 21.6 ^l |
| ArC ⁺ (⁴ Σ ⁻) → Ar(¹ S) + C ⁺ (⁴ P) | 74.5 | 73.5 | | |
| ArC ⁺ (⁴ Σ ⁻) → Ar ⁺ (² P) + C(³ P) | 56.5 | 55.0 | 49.1 ^l | |
| ArN ⁺ (X ³ Σ ⁻) → Ar(¹ S) + N ⁺ (³ P) | 48.7 | 48.0 | 30 ^f | 53.0 ^f |
| ArO ⁺ (X ⁴ Σ ⁻) → Ar(¹ S) + O ⁺ (⁴ S) | 10.0 | 9.6 | 15.4 ⁿ | 15.7 ^m |
| ArO ⁺ (² Π) → Ar(¹ S) + O ⁺ (² D) | 75.4 ^a | 74.1 ^a | | |
| ArO ⁺ (² Π) → Ar ⁺ (² P) + O(³ P) | 50.5 | 49.2 | 41.5; ^b 39.2 ^p | |
| ArF ⁺ (X ¹ Σ ⁺) → Ar(¹ S) + F ⁺ (¹ D) | 139.1 ^b | 138.0 ^b | | |
| ArF ⁺ (X ¹ Σ ⁺) → Ar ⁺ (² P) + F(² P) | 49.6 ^e | 48.2 ^e | 69.6 ^g | >38.1 ^e |
| ArF ⁺ (³ Π) → Ar(¹ S) + F ⁺ (³ P) | 53.0 | 52.4 | | |
| ArF ⁺ (³ Π) → Ar ⁺ (² P) + F(² P) | 16.6 | 16.0 | | |
| ArNe ⁺ (X ² Σ ⁺) → Ar(¹ S) + Ne ⁺ (² P) | 134.6 | 134.4 | | |
| ArNe ⁺ (X ² Σ ⁺) → Ar ⁺ (² P) + Ne(¹ S) | 1.8 | 1.6 | 1.92; ^d 1.96; ^h 1.82 ^q | |

^a Calculated by using the atomic ground states and the experimentally derived³² excitation energy O⁺(⁴S) → O⁺(²D) (76.6 kcal/mol). ^b Calculated by using the atomic ground states and the experimentally derived³² excitation energy F⁺(³P) → F⁺(¹D) (59.6 kcal/mol). ^c Reference 18. ^d Reference 15f. ^e D₀ value, ref 14a. ^f Estimated value in ref 7b. ^g Reference 7c. ^h Reference 15g. ⁱ Reference 10a. ^j Reference 10b. ^k Reference 18a. ^l Reference 12a. ^m Reference 13b. ⁿ Reference 13a. ^o Reference 8k. ^p Reference 7b. ^q D₀ value, ref 15i. ^r Reference 11. ^s Calculated by using isogyric reactions; see text.

Theoretical Methods

The theoretical methods used to investigate ions NeX⁺ and ArX⁺ are the same as described in I for the study of HeX⁺ and may be taken from there.

Results

Tables I and II show our theoretically predicted equilibrium distances, total energies, vibrational frequencies, corresponding ZPE data, and BSSE corrections for the NeX⁺ and ArX⁺ cations, respectively. The tables also show the calculated energies for the atomic fragments of the dissociation reactions. The dissociation energies D_e and D₀ for the spin- and space-symmetry-allowed reactions are listed in Charts I and II together with representative earlier theoretical and experimental results.

NeLi⁺ and ArLi⁺. The interaction potentials between Li⁺ and Ne or Ar in their electronic ground states have been determined

quite accurately by molecular beam scattering experiments.^{8k,m} The experimentally determined D_e values for NeLi⁺ (2.6 kcal/mol)^{8k} and ArLi⁺ (7.0 and 7.2 kcal/mol)^{8k,m} shown in Chart I are in good agreement with our calculations which for NeLi⁺ predict D_e = 3.0 kcal/mol, while for ArLi⁺ a slightly too small dissociation energy of D_e = 5.7 kcal/mol is calculated. Earlier theoretical studies based on ab initio^{8a} calculations or the electron-gas approximation^{8b-h} are generally in accord with these data predicting dissociation energies for NeLi⁺ of D_e = 2.8 kcal/mol^{8b-d} and for ArLi⁺ D_e values between 6.2 kcal/mol^{7a} and 10.3 kcal/mol.^{8b,c} Our theoretically determined equilibrium distances r_e for NeLi⁺ (2.032 Å) and ArLi⁺ (2.383 Å) are slightly shorter than the experimentally^{8k} observed values of 2.11 and 2.42 Å, respectively. The good agreement of our calculated results with the experimentally derived data indicates that the theoretical level employed in our study is capable of producing reliable predictions for weakly interacting systems such as NeLi⁺ and ArLi⁺.

NeBe⁺ and ArBe⁺. The data in Tables I and II show that the interatomic distance in NeBe⁺ is slightly longer than in NeLi⁺, while r_e of ArBe⁺ is shorter than that of ArLi⁺. Accordingly, the dissociation energy for NeBe⁺ is smaller than for that for NeLi⁺. The opposite result is found for ArBe⁺, which has a D_e value of respectable 10.9 kcal/mol, nearly twice the value predicted for ArLi⁺. The calculated dissociation energy for the ground state of ArBe⁺ is in very good agreement with experimentally derived¹⁰ values of 11.5–13.0 kcal/mol.

(15) (a) Cohen, J. S.; Schneider, B. *J. Chem. Phys.* **1974**, *61*, 3230; (b) Kuntz, P. J.; Doran, M.; Hillier, I. H. *Chem. Phys.* **1979**, *43*, 197. (c) Gilbert, T. L.; Wahl, A. C. *J. Chem. Phys.* **1971**, *65*, 5247. (d) Michels, H. H.; Hobbs, R. H.; Wright, L. A. *J. Chem. Phys.* **1978**, *68*, 5151. (e) Wadt, W. *J. Chem. Phys.* **1980**, *73*, 3915. (f) Hausamann, D.; Morgner, H. *Mol. Phys.* **1985**, *54*, 1085. (g) Brunetti, B.; Vecchiocattivi, F.; Aguilar-Navarro, A.; Sole, A. *Chem. Phys. Lett.* **1986**, *126*, 245. (h) Frommhold, L.; Biondi, M. A. *Phys. Rev.* **1969**, *185*, 244. (i) Pratt, S. T.; Dehmer, P. M. *J. Chem. Phys.* **1982**, *76*, 3433.

TABLE II: Calculated Bond Lengths, r_e (Å), Total Energies, E_{tot} (hartrees), Vibrational Frequencies, ν (cm⁻¹), Zero-Point Vibrational Energies, ZPE, and Basis Set Superposition Errors, BSSE (kcal/mol), of ArX⁺ Ions

| struct | sym | MP2/6-31G(d,p) | | | | MP4/6-311G(2df,2pd) | | |
|-------------------|-------------------------------|----------------|------------------|-------|-----|---------------------|------------------------|------------------------------------|
| | | r_e | E_{tot} | ν | ZPE | r_e | E_{tot} | BSSE |
| ArLi ⁺ | X ¹ Σ ⁺ | 2.441 | -534.1663 | 252 | 0.4 | 2.383 | -534.2781 | 1.2 |
| ArBe ⁺ | X ² Σ ⁺ | 2.045 | -541.2154 | 382 | 0.5 | 2.104 | -541.3273 | 1.5 |
| ArB ⁺ | X ¹ Σ ⁺ | 2.738 | -551.1966 | 112 | 0.2 | 2.427 | -551.3312 | 0.8 |
| ArB ⁺ | ³ Π | 1.847 | -551.0924 | 553 | 0.8 | 1.856 | -551.2146 | 1.8 |
| ArC ⁺ | X ² Π | 2.059 | -564.2777 | 302 | 0.4 | | -564.4287 ^c | 1.3 |
| ArC ⁺ | ¹ Σ ⁻ | 1.723 | -564.1900 | 712 | 1.0 | | -564.3265 ^c | 1.9; ^a 1.6 ^b |
| ArN ⁺ | X ³ Σ ⁻ | 1.836 | -580.9185 | 507 | 0.7 | | -581.0872 ^c | 1.7 |
| ArO ⁺ | X ⁴ Σ ⁻ | 2.292 | -601.3383 | 258 | 0.4 | | -601.5238 ^c | 0.9 |
| ArO ⁺ | ² Π | 1.665 | -601.3068 | 909 | 1.3 | | -601.5079 ^c | 2.1; ^a 2.2 ^b |
| ArF ⁺ | X ¹ Σ ⁺ | 1.637 | -625.9122 | 750 | 1.1 | | -626.1402 ^c | 2.8 |
| ArF ⁺ | ³ Π | 2.120 | -625.8745 | 391 | 0.6 | | -626.0955 ^c | 1.3 |
| ArNe ⁺ | X ² Σ ⁺ | 2.410 | -654.9891 | 151 | 0.2 | | -655.2504 ^c | 1.1 |
| Ar | ¹ S | | -526.9200 | | | | -527.0313 | |
| Ar ⁺ | ² P | | -526.3560 | | | | -526.4590 | |
| C | ³ P | | -37.7365 | | | | -37.7748 | |
| O | ³ P | | -74.8820 | | | | -74.9648 | |
| F | ² P | | -99.4890 | | | | -99.6079 | |

^aDissociation into Ar⁺ + X. ^bDissociation into Ar + X⁺. ^cAt MP2/6-31G(d,p) optimized geometries.

NeB⁺ and ArB⁺. The noble-gas boron cations NeB⁺ and ArB⁺ are predicted by our calculations to be very weakly bound in their respective X¹Σ⁺ ground states, namely, $D_e = 1.2$ kcal/mol for NeB⁺ and $D_e = 5.6$ kcal/mol for ArB⁺. The first excited ³Π states of both species are calculated to be significantly stronger bound especially in case of ArB⁺. The theoretical values shown in Charts I and II are $D_e = 7.3$ and 35.2 kcal/mol for NeB⁺(³Π) and ArB⁺(³Π), respectively. Our results for ArB⁺ agree with the experimental values of Ding et al.^{11b} for $D_e = 6.9$ and 34.6 kcal/mol for the X¹Σ⁺ and ³Π states. The experimental study^{11b} reports the lack of an oscillatory structure for the scattering of B⁺ on Ne indicating very weak interactions. In the same paper SCF results for ground and excited states of NeB⁺ and ArB⁺ have been reported which gave much lower D_e values for the X¹Σ⁺ state (0.5 kcal/mol (NeB⁺); 2.1 kcal/mol (ArB⁺)) and ³Π state (1.6 kcal/mol (NeB⁺); 27.7 kcal/mol (ArB⁺)) than our results. A later ab initio SCF-CI study by Iwata and Sato^{11a} predicts larger binding energies, i.e., 3.7 and 6.5 kcal/mol for NeB⁺ in its X¹Σ⁺ and ³Π states and 8.1 and 38.5 kcal/mol for the respective ArB⁺ states.

NeC⁺ and ArC⁺. The carbon analogues of the NgX⁺ series have been calculated in their X²Π ground states and ⁴Σ⁻ excited states. Like the NgB⁺ states discussed above, there is a substantial increase in the bond strength from the X²Π ground state to the ⁴Σ⁻ excited state of NeC⁺ and ArC⁺. Our theoretically predicted D_e values for NeC⁺ are 3.0 kcal/mol (X²Π) and 21.7 kcal/mol (⁴Σ⁻). A previous CASSCF investigation^{12b} of NeC⁺ predicts weaker binding energy ($D_e < 0.2$ kcal/mol) for the X²Π ground state. It will be difficult to observe NeC⁺ experimentally in its X²Π ground state, but the ⁴Σ⁻ state should be observable in the gas phase. Excited states of NeC⁺ which dissociate into Ne⁺ + C have recently been detected by Jonathan et al.^{12c}

In contrast to NeC⁺, the ²Π ground state of ArC⁺ is calculated with a substantial dissociation energy $D_e = 20.6$ kcal/mol, which is in perfect agreement with the experimental value of $D_e = 21.6$ kcal/mol reported by Hillier et al.^{12a} They also report CI calculations for ArC⁺ predicting a dissociation energy $D_e = 27.2$ kcal/mol for ArC⁺(X²Π). Like NeC⁺, the excited ⁴Σ⁻ state of ArC⁺ possesses a larger dissociation energy than the ground state. However, unlike NeC⁺, the lowest lying dissociation limit of (⁴Σ⁻) ArC⁺ yields the noble-gas cation and neutral carbon, i.e., Ar⁺(²P) + C(³P) (Chart II). Our calculated result for the binding energy of this state ($D_e = 56.5$ kcal/mol) is in reasonable agreement with the SCF-CI data ($D_e = 49.1$ kcal/mol) reported by Hillier et al.^{12a} It seems possible that the observed ArC⁺ species reported by Jonathan et al.^{12c} that dissociates into Ar⁺ + C corresponds to the ⁴Σ⁻ state.

NeN⁺ and ArN⁺. The nitrogen analogues NeN⁺ and ArN⁺ have been calculated only in their X³Σ⁻ state. Our previous study of HeX⁺ cations (I) included also the excited ³Π state, which

exhibits a much shorter interatomic distance and stronger binding than the X³Σ⁻ state. Because of convergence difficulties in the optimization of the ³Π states of NeN⁺ and ArN⁺, we report only the results for the X³Σ⁻ ground states.

NeN⁺(X³Σ⁻) is predicted to have a dissociation energy D_e of 9.2 kcal/mol. The earlier Hartree-Fock calculation by Liebman and Allen^{7b} gave a value for $D_e = 2.3$ kcal/mol, which is too low. Of all the NeX⁺ systems with X = Li-F, NeN⁺ has the strongest bound ground state. An explanation for this finding, which is analogous to the HeX⁺ first-row cations (I), is given below under Discussion. The clearly stronger binding of NeN⁺ than for NeC⁺ and NeO⁺ in their respective ground states has been suggested^{1a} as an explanation why charge-stripping experiments of these ions as precursors yield only the doubly charged cation NeN²⁺, while no NeC²⁺ and NeO²⁺ could be observed.^{12c} For NeN⁺, but not for NeC⁺ and NeO⁺, a significant population of the electronic ground state is possible due to the stronger binding. If only the ground state of the singly charged cations has a favorable Franck-Condon overlap with the respective doubly charged species, it becomes comprehensive why only NeN²⁺ was detected.

The experimental results for the argon analogues reported in the same paper^{12c} can be understood in the same fashion. Our calculated results shown in Chart II predict that ArN⁺ also has the largest dissociation energy of all ArX⁺ cations in their ground states (using isogyric reactions, the D_e value of ArF⁺, however, is slightly higher; see Discussion). The dissociation energy for (X³Σ⁻) ArN⁺ $D_e = 48.7$ kcal/mol indicates substantially stronger binding interactions than for (X²Π) ArC⁺ ($D_e = 20.6$ kcal/mol) and (X⁴Σ⁻) ArO⁺ ($D_e = 10.0$ kcal/mol). Only ArN⁺, but not ArC⁺ and ArO⁺, yielded charge-stripping signals of sufficient intensity to allow an estimate of the ionization energy.^{12c} The population of the electronic ground state of ArN⁺ can be expected to be much higher than the ground states of ArC⁺ and ArO⁺ because the latter are much weaker bound. ArN⁺ has been the subject of a Hartree-Fock calculation which predicted a dissociation energy D_e of only ca. 30 kcal/mol.^{7b} In the same paper an estimate of the stability of ArN⁺ using a thermochemical cycle based on experimental data gave an estimate for $D_e = 53.0$ kcal/mol, which is in reasonable agreement with our computed value of 48.3 kcal/mol.

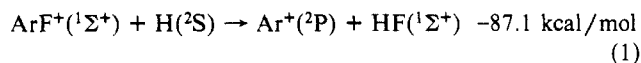
NeO⁺ and ArO⁺. The predicted dissociation energy D_e for the ground X⁴Σ⁻ state of NeO⁺ (1.2 kcal/mol) indicates very weak binding. The excited ²Π state is calculated to be somewhat stronger bound with a D_e value of 6.3 kcal/mol (Chart I). These values are similar to the X¹Σ⁺ ground state and ³Π excited state of NeB⁺. As for NeB⁺,^{11b} scattering experiments of O⁺ in several electronic states with Ne did not yield any detectable structure in the differential cross section^{13a} indicating essentially repulsive potentials. The argon analogue ArO⁺ is calculated to be stronger bound than NeO⁺. Our theoretical value for the dissociation

energy D_e of the $X^4\Sigma^-$ ground state is 10.0 kcal/mol. The experimentally derived value from scattering data¹³ is $D_e = 15.7$ kcal/mol, and a POL-CI calculation of the $X^4\Sigma^-$ state gave $D_e = 15.4$ kcal/mol.^{13a} The considerably stronger bound $^2\Pi$ state of ArO^+ dissociates into $\text{Ar}^+(^2P) + \text{O}(^3P)$ with a calculated D_e value of 50.5 kcal/mol (Chart II). There are no experimental values available for the $^2\Pi$ state of ArO^+ , but our result of a higher dissociation energy than in the ground state is in agreement with earlier ab initio data which give D_e values of 41.5 kcal/mol^{13a} and 39.2 kcal/mol.^{7b}

NeF⁺ and ArF⁺. Gas-phase-ion experiments by Berkowitz and Chupka^{12a} searching for noble-gas fluoride ions yielded ArF^+ while all attempts to detect HeF^+ and NeF^+ failed. Thermodynamic calculations of the investigated reactions allowed an estimate for the dissociation energy for the ground state of ArF^+ as $D_0 \geq 38.1$ kcal/mol.^{14a} Recently, measurements of inelastic collisions of F^+ with Ne and ab initio calculations of NeF^+ have been reported by Hottoka et al.^{14b} A mass-39 peak was observed that may correspond to NeF^+ , but the signal intensity was too low to allow for experiments that would corroborate this assignment.^{14b}

Our calculated data for NeF^+ indicate weak binding ($D_e = 3.6$ kcal/mol) for the $X^3\Pi$ ground state. The CASSCF results of Hottoka et al.^{14b} predict a purely repulsive potential, while their D_e value for the $^1\Sigma^+$ excited state of NeF^+ (37.9 kcal/mol) is in excellent agreement with our result (39.8 kcal/mol). The earlier Hartree-Fock calculation of Liebman and Allen^{7a} gives a value that is too low (30 kcal/mol).

ArF^+ differs from NeF^+ for two reasons. First, ArF^+ has a $X^1\Sigma^+$ ground state, and second, the lowest lying dissociation limit for ArF^+ yields neutral fluorine, i.e., $\text{Ar}^+(^2P) + \text{F}(^2P)$. The argon fluoride cation ArF^+ is a unique species because, within our series NgX^+ , it is the only example where the ionization energy of X is higher than Ng (IE(F) = 17.422 eV; IE(Ar) = 15.759 eV).⁶ The rather high dissociation energy of ArF^+ in its $^1\Sigma^+$ ground state let it seem possible that a salt compound of ArF^+ with a suitable anion might be stable. The experimental aspects of this proposal have recently been discussed,^{1b} and it was concluded that molecules such as $\text{ArF}(\text{AuF}_6)$ or $\text{ArF}(\text{SbF}_6)$ could perhaps be synthesized. Because the dissociation reaction of $\text{ArF}(X^1\Sigma^+)$ in $\text{Ar}^+(^2P) + \text{F}(^2P)$ is not isogyric,¹⁶ the error in the calculated D_e value might be higher than the other reactions which are isogyric. In order to assess the dissociation energy of ($X^1\Sigma^+$) ArF^+ more reliably, we calculated the reaction energy of the isogyric reaction 1 at MP4(SDTQ)/6-311G(2df,2pd)//MP2/6-31G(d,p) + ZPE:¹⁷



The calculated reaction energy of -87.1 kcal/mol for reaction 1 combined with the experimentally derived dissociation energy D_0 for HF (135.3 kcal/mol)¹⁸ gives a bond dissociation energy for $\text{ArF}^+(X^1\Sigma^+)$ $D_0 = 48.2$ kcal/mol. At the same level of theory the dissociation energy of isoelectronic ClF using the analogous reaction to 1, D_0 , is calculated as 58.1 kcal/mol.^{1b} The experimental value for ClF is $D_0 = 60.3$ kcal/mol.¹⁸ Therefore, we estimate the dissociation energy D_0 of ArF^+ in its $X^1\Sigma^+$ ground state as 50 ± 3 kcal/mol. The Hartree-Fock value reported earlier by Liebman and Allen^{7c} ($D_e = 69.6$ kcal/mol) is too high. The $^3\Pi$ excited state of ArF^+ is predicted to be significantly weaker bound. The calculated value for D_e is 16.6 kcal/mol and for D_0 it is 16.0 kcal/mol (Chart II).

NeNe⁺ and ArNe⁺. Our theoretically predicted result for the dissociation energy D_e of NeNe^+ (29.8 kcal/mol) is nearly in perfect agreement with the experimental values of $D_e = 30.0$ kcal/mol¹⁸ and 31.1 kcal/mol.^{15h} Other theoretical studies report

(16) Pople, J. A.; Frisch, M. J.; Luke, B. T.; Binkley, J. S. *Int. J. Quantum Chem. Quantum Chem. Symp.* **1983**, *17*, 307.

(17) The calculated total energy of HF at MP4(SDTQ)/6-311G(2df,2pd)//MP2/6-31G(d,p) is -100.3270 hartrees at the equilibrium distance $r_e = 0.921$ Å. The ZPE correction for HF is 5.6 kcal/mol, and the total energy of the hydrogen atom is -0.4998 hartrees.^{1b}

(18) Huber, K. P.; Herzberg, G. *Constants of Diatomic Molecules*; Van Nostrand Reinhold: New York, 1979.

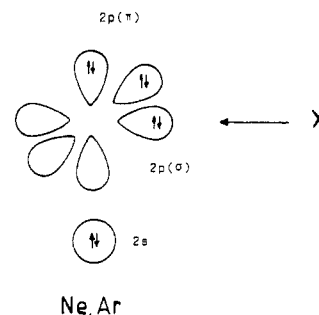


Figure 1. Schematic representation of the valence orbitals of Ne and Ar upon approach of X^+ .

TABLE III: Theoretically Predicted Dissociation Energies, D_e , and Charge-Induced Dipole Interaction Energies, E_{ind} , Using Eq 2 for the Ground States of HeX^+ , NeX^+ , and ArX^+ (kcal/mol)

| X | D_e | | | E_{ind} | | |
|----|-----------------|------|------|-----------------|-----|------|
| | He ^a | Ne | Ar | He ^a | Ne | Ar |
| Li | 1.5 | 3.0 | 5.7 | 1.9 | 3.8 | 8.4 |
| Be | 0.3 | 0.9 | 10.9 | 0.4 | 3.7 | 13.9 |
| B | 0.5 | 1.2 | 5.6 | 0.5 | 1.6 | 7.8 |
| C | 1.1 | 3.0 | 20.6 | 1.0 | 3.5 | 15.1 |
| N | 4.1 | 9.2 | 48.7 | 3.6 | 6.7 | 23.9 |
| O | 0.8 | 1.2 | 10.0 | 0.9 | 2.5 | 9.9 |
| F | 1.4 | 3.6 | 49.6 | 1.7 | 4.4 | 12.9 |
| Ne | 10.4 | 29.8 | 1.8 | 8.7 | 7.5 | 1.9 |

^a Values taken from ref 2.

similar values of 33.2 kcal/mol^{15b} and 31.1 kcal/mol.^{15d} The argon analogue ArNe^+ is only very weakly bound. Our calculated result of $D_e = 1.8$ kcal/mol matches the experimentally derived data of 1.96^{15g} and 1.82 kcal/mol.¹⁵ⁱ

Discussion

After presenting our calculated results for the binding energies of NeX^+ and ArX^+ cations in their ground and selected excited states, we now discuss the trends in the binding energies when going from $X = \text{Li}$ to $X = \text{Ne}$. The discussion is analogous to the presentation in I, and we compare the calculated data for HeX^+ , NeX^+ , and ArX^+ .

The triply degenerate HOMO of Ne (2p orbital) and Ar (3p orbital) splits into a set of doubly degenerate $p(\pi)$ orbitals and a $p(\sigma)$ AO when approached by an ion X^+ (Figure 1). The valence AOs of first-row atomic ions X^+ consist of the 2s AO and the 2p AOs, which also split upon approach of Ne or Ar into a $p(\sigma)$ orbital and a degenerate $p(\pi)$ AO. Because the overlap of the $p(\sigma)$ AO of Ng with the respective σ orbital of X^+ is larger than overlap of the π orbitals, the dominant interactions will involve σ -type orbitals. A schematic representation of the atomic orbitals of X^+ is shown in Figure 2 of I.

In order to facilitate the comparison of interaction energies, we have listed in Table III the calculated dissociation energies D_e of the first-row cations HeX^+ , NeX^+ , and ArX^+ in their electronic ground states. For the HeX^+ and NeX^+ cations, the trend in the D_e values from $X = \text{Li}$ to Ne is the same with NeX^+ always being more strongly bound. The trend in the dissociation energies of ArX^+ cations is similar, with two exceptions. One exception is $\text{ArBe}^+(X^2\Sigma^+)$, which is more strongly bound than $\text{ArLi}^+(X^1\Sigma^+)$ and $\text{ArB}^+(X^1\Sigma^+)$, while in the case of the neon and helium analogues NgBe^+ is calculated with the lowest D_e value. As discussed in I, frontier orbital interactions in NgBe^+ involve the singly occupied 2s AO of $\text{Be}^+(^2S)$. HOMO-SOMO interactions may become attractive with better donors, while they may be repulsive with poor donors.¹⁹ Argon is a significantly better donor than neon and helium, which causes a change in the trend in dissociation energy from NgLi^+ to NgBe^+ . The better donor

(19) Bernardi, F.; Epitiotis, N. D.; Cherry, W.; Schlegel, H. B.; Whangbo, M.-H.; Wolfe, S. J. *Am. Chem. Soc.* **1976**, *98*, 469.

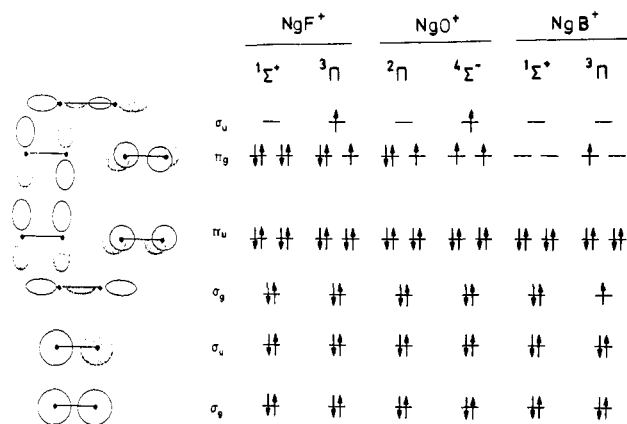


Figure 2. Schematic representation of the valence orbitals of NgX^+ ions in the ground and excited state.

ability of Ar than that of Ne and He is evident by the strong increase in the dissociation energy D_e for a given NgX^+ (for the apparent exception ArNe^+ see below). The difference in the D_e values between ArX^+ and NeX^+ is much higher than the change from NeX^+ to HeX^+ (Table III). This is caused by the differences in ionization energy and dipole polarizability α of Ng atoms, which are clearly larger between Ar and Ne than between Ne and He (IE(He) = 24.587 eV, IE(Ne) = 21.564 eV, IE(Ar) = 15.759 eV; $\alpha(\text{He}) = 0.205 \text{ \AA}^3$, $\alpha(\text{Ne}) = 0.395 \text{ \AA}^3$, $\alpha(\text{Ar}) = 1.64 \text{ \AA}^3$).^{6,20}

The second exception concerns ArNe^+ . The very weakly bound $X^2\Sigma^+$ ground state of ArNe^+ is comprehensible as the result of donor-acceptor interactions between the poor electron donor Ne(¹S) and Ar(²P). This explains why ArNe^+ is the only example of our ArX^+ series that has a lower dissociation energy in its ground state than the respective NeX^+ and even HeX^+ analogues. Comparing donor-acceptor interactions of NeNe^+ with ArNe^+ in their $X^2\Sigma^+$ ground states shows that the acceptor atom Ne(²P) in the former diatomic is replaced by the poorer acceptor atom Ar(²P) yielding much weaker binding. ArNe^+ is only formally a member of the ArX^+ first-row sweep. Considering the dissociation products, it belongs to the NeX^+ (X = Ar) cations.

Thus, the NeX^+ and ArX^+ ground states exhibit the same trend in D_e values as the HeX^+ analogues, and the trend as well as the exceptions (ArBe^+ , ArNe^+) can be understood within the donor-acceptor model as discussed in I. Also the differences for the excited states of NeX^+ and ArX^+ can be rationalized in the same way as discussed in I for HeX^+ . The results shown in Chart I and Chart II show that the dissociation energy for the excited states is always higher than that for the ground state of NeX^+ and ArX^+ . The same result had been found for the corresponding states of HeX^+ , which could be rationalized by the better acceptor ability of the corresponding excited state of X^+ (see I). Convergence difficulties at the MP2/6-31G(d,p) level did not allow the optimization of the $^2\Pi$ states of NeBe^+ and ArBe^+ and the $^3\Pi$ states of NeN^+ and ArN^+ . Preliminary CASSCF calculations^{21a} indicate significantly stronger interactions for the excited states compared with the ground states. For the $^2\Pi$ state of ArBe^+ experimental D_e values of 39.7–47.7 kcal/mol have been reported.¹⁰

The argon analogues ArF^+ and ArNe^+ exhibit fundamental differences compared with NeF^+ and NeNe^+ , not only because Ar has a lower ionization energy than F and Ne in the respective atomic ground state. Also, unlike NeF^+ , ArF^+ has a $^1\Sigma^+$ ground state and $^3\Pi$ excited state which can best be understood by considering the molecular orbitals of the ArF^+ molecule rather than the atomic orbitals of the atoms. The valence MOs of ArF^+ are schematically shown in Figure 2.

In the $^1\Sigma^+$ state there are three doubly occupied σ orbitals and two degenerate π MOs occupied by eight electrons. In the $^3\Pi$ state of ArF^+ one electron is excited from the antibonding π_g MO

to the highest lying σ_u valence MO which is strongly antibonding (Figure 2). The result that the $^3\Pi$ state of ArF^+ is both more weakly bound and energetically higher lying than the $^1\Sigma^+$ state indicates that ArF^+ is the first example in our series for a molecule which is determined by the bonding and antibonding character of the molecular orbitals rather than the HOMO-LUMO interactions of the respective atoms. For example, ArO^+ should have a $^2\Pi$ ground state rather than $^4\Sigma^-$ when the MOs of the two electronic states are considered (Figure 2). Also, while the molecular orbitals of the 15-valence electron system ArO^+ still correctly predict that the $^4\Sigma^-$ state should have a smaller D_e value than the $^2\Pi$ state, it fails for other systems. Figure 2 also shows the molecular orbitals for ArB^+ . Excitation of one electron from the doubly occupied σ_g AO to the antibonding π_g AO should yield weaker interactions in the $^3\Pi$ state. The opposite holds true; $^3\Pi$ ArB^+ has a substantially higher D_e value than the $^1\Sigma^+$ state (Chart II). The reason for this is that the weakly bound systems are not well described by the molecular orbitals but rather by the electronic structure of the constituting atoms.

What is the physical origin of the binding in NeX^+ and ArX^+ cations in their ground states? We calculated the charge-induced dipole interactions E_{ind} at their equilibrium distances r_e using eq²² 2:

$$E_{\text{ind}} = -0.5\alpha q^2 r_e^{-4} \quad (2)$$

Using the recommended²⁰ electric dipole polarizabilities $\alpha(\text{Ne}) = 0.395 \text{ \AA}^3$, $\alpha(\text{Ar}) = 1.64 \text{ \AA}^3$ and $\alpha(\text{F}) = 0.557 \text{ \AA}^3$, we calculated E_{ind} values for NeX^+ and ArX^+ cations in their ground states. The results are shown in Table III, together with the data for HeX^+ taken from I. A comparison of the D_e values and E_{ind} results reveals remarkably similar data for all HeX^+ and most NeX^+ and ArX^+ cations. From the NeX^+ species, only NeNe^+ exhibits a significantly larger D_e value than E_{ind} , which suggests some chemical interactions. Electron interactions are also clearly indicated for ArN^+ and ArF^+ and possibly to a small degree in ArC^+ . All other NgX^+ cations in their ground states are predominantly bound by charge-induced dipole interactions. In order to check the validity of our conclusion, we calculated the atomic polarizability of Ne and Ar at the MP4(SDTQ)/6-311G(2df,2pd) level. Similar to helium,² we found^{21b} that the calculated values for $\alpha(\text{Ne})$ and $\alpha(\text{Ar})$ are in very good agreement with the recommended²⁰ values. For those NgX^+ cations that are bound by charge-induced dipole interactions, the differences in E_{ind} and r_e are primarily caused by the different ionic radii of X^+ .

Why is it possible that the model of frontier orbital interactions can be used to rationalize the bonding features of noble-gas cations HeX^+ , NeX^+ , and ArX^+ when the physical origin of the binding interactions are mainly charge-induced dipole forces? The answer is not difficult. If the charge distribution of the atomic ions X^+ would be isotropical, the interactions with a noble-gas atom Ng would be nearly the same for all NgX^+ cations, with small variations caused by the different polarizabilities of X^+ . The differences in the equilibrium distances and binding energies among the various NgX^+ species are mainly caused by the anisotropy of the electronic density distribution. This is nicely reflected by the Laplace concentration of $-\nabla^2\rho(\mathbf{r})$. Figure 3 gives a perspective drawing and a contour line diagram of the Laplace concentration of $\text{NeN}^+(X^3\Sigma^-)$ in the xz plane with the z axis being parallel to the Ne_eN bond axis. In the valence shell of the N atom, negative charge is concentrated (indicated by dashed lines in the contour line diagram) in regions, in which one expects the $2p_x$ electron.²³ Along the z axis in the direction of the Ne atom, there is a deep hole in the valence shell concentration of the N atom (Figure 3). It is this hole that imparts stronger acceptor ability to N^+ .

(22) Equation 2 describes only the leading term in the multipole expansion for the electrostatic interactions which, however, can be assumed to be the dominant term: Buckingham, A. D.; Fowler, P. W.; Hutson, J. M. *Chem. Rev.* **1988**, *88*, 963.

(23) The same holds for the $2p_y$ electron. Hence, there is a torus of negative charge concentration at N perpendicular to the Ne_eN axis that can be verified by plotting the Laplace concentration in the yz or other planes containing the internuclear axis.

(20) Miller, T. M.; Bederson, B. *Adv. At. Mol. Phys.* **1977**, *13*, 1.

(21) (a) Frenking, G.; Koch, W. to be published. (b) Collins, J. R.; Frenking, G. to be published.

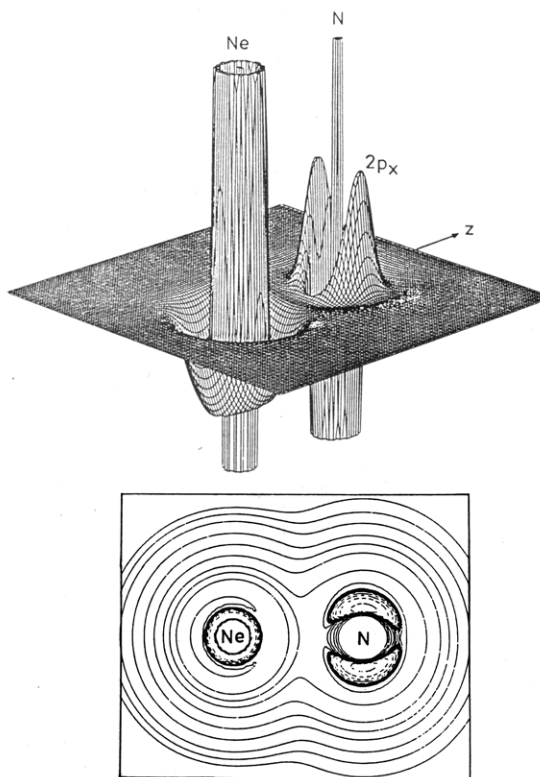


Figure 3. Perspective drawing (above) and contour line diagram (below) of the Laplace concentration $-\nabla^2\rho(\mathbf{r})$ of $\text{NeN}^+(\text{X}^3\Sigma^-)$. Dashed contour lines are in regions of concentration of negative charge, and solid contour lines are in regions of charge depletion. Inner-shell concentrations are not shown in the contour line diagram (HF/6-31G(d) calculations).

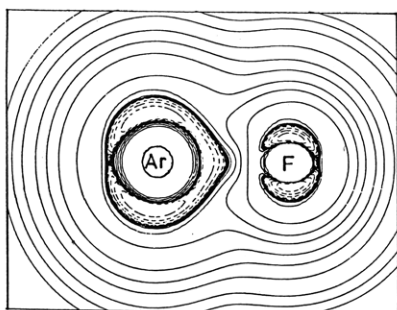


Figure 4. Contour line diagram of the Laplace concentration $-\nabla^2\rho(\mathbf{r})$ of $\text{ArF}^+(\text{X}^1\Sigma^+)$. Dashed contour lines are in regions of concentration of negative charge, and solid contour lines are in regions of charge depletion. Inner-shell concentrations are not shown in the contour line diagram (HF/6-31G(d) calculations).

Electrons of Ne are dragged toward the concentration hole at N in a similar way as has been analyzed for the helium compounds discussed in I and in ref 3. Donor-acceptor interactions for most of the cations NgX^+ investigated in this work are not that strong as for the helium-carbon dications, for which substantial charge concentrations in the internuclear region reveal the formation of a semipolar covalent HeC bond.³ For example, the distortion of the valence shell of Ne can only be observed by a closer inspection of Figure 3: negative charge is more depleted from the nonbonding side of Ne than from the side facing the N atom.

The distortion of the valence shell of Ng is more visible in the case of $\text{ArF}^+(\text{X}^1\Sigma^+)$ (Figure 4). Negative charge of Ar is polarized toward the concentration hole at F that is larger at the bonding than at the nonbonding side. It is noteworthy that the Laplace concentration at Ar adopts a pattern that is similar to that of F. This suggests an electron transfer from Ar to F^+ and covalent bonding between Ar^+ and F in the sense discussed above.

Any transfer of negative charge from Ng to X^+ can be made visible by plotting the difference electron density distribution $\Delta\rho(\mathbf{r})$ of NgX^+ . For this purpose, the density distribution of the pro-

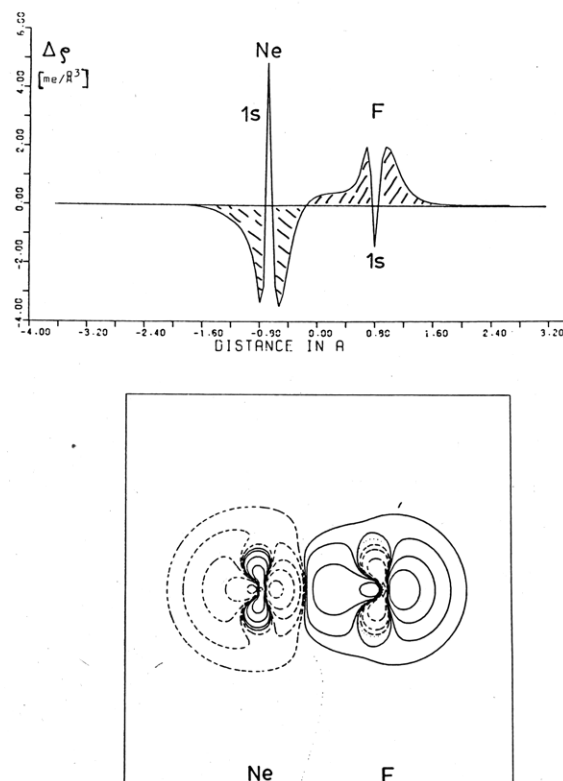


Figure 5. Profile plot along the internuclear axis (above) and contour line diagram (below) of the difference electron density $\Delta\rho(\mathbf{r}) = \rho(\mathbf{r})^{\text{molecule}} - \rho(\mathbf{r})^{\text{promolecule}}$ calculated for $\text{NeF}^+(\text{X}^1\Sigma^+)$ (HF/6-31G(d) calculations).

molecule, which is formed by the noninteracting atoms in the geometry of the molecule, is subtracted from that of NgX^+ . Figure 5 gives a profile plot and a contour line diagram of $\Delta\rho(\mathbf{r})$ of NeF^+ , which both show that electron density is transferred from Ne to F^+ . It accumulates in the bonding and nonbonding region of F^+ . In this way, Ne becomes partially positive while F^+ loses some of its positive charge. As a consequence, negative charge residing in the $2p(\pi)$ or $1s$ orbitals, which are not involved in the charge transfer from Ne to F^+ , is contracted toward the Ne nucleus but shifted away from the F nucleus. Hence, $\Delta\rho(\mathbf{r})$ is positive (negative) in the region of the $2p(\pi)$ and $1s$ orbitals of Ne ($2p(\pi)$ and $1s$ orbitals of F). This confirms that both electrostatic interactions and charge transfer from Ng to X^+ contribute to the stability of ions NgX^+ . It remains to be seen whether this charge transfer establishes a covalent bond between Ng and X^+ .

As discussed in I, the Laplace concentration of NgX^+ does not reveal covalent bonding. However, necessary and sufficient conditions for covalent bonding have been suggested by Cremer and Kraka^{24,25} as follows: (a) There must be a path of maximum electron density (MED path) between the atoms in question (necessary condition for covalent bonding). A MED path implies a saddle point \mathbf{r}_b and an interatomic surface separating the basins of the two atoms. (b) The energy density $H(\mathbf{r})$ must be < 0 at \mathbf{r} , thus indicating that electron density at \mathbf{r}_b stabilizes the system (sufficient condition for covalent bonding). Our classification if the NgX^+ cations are covalently bound or if the interactions are caused by charge interactions is based on these criteria.

Table IV gives the position of the saddle point \mathbf{r}_b , the electron density ρ_b , the Laplace value $\nabla^2\rho_b$, and the energy density H_b calculated at the HF/6-31G(d,p) level. There is a linear relationship between the distance of \mathbf{r}_b from Ng and the magnitude of ρ_b . The closer \mathbf{r}_b at Ng is, the larger the electron density ρ_b is. *There is no relationship between ρ_b and the electronegativity of X.*²⁶ For example, in the ground state of NgX^+ the value of

(24) Cremer, D.; Kraka, E. In *Conceptual Approaches in Quantum Chemistry—Models and Applications*. *Croat. Chem. Acta* **1984**, *57*, 1259.

(25) Cremer, D.; Kraka, E. *Angew. Chem.* **1984**, *96*, 612; *Angew. Chem., Int. Ed. Engl.* **1984**, *23*, 627.

TABLE IV: Nature of the Ng,X Interactions As Described by the Properties of the Electron Density Distribution Calculated at the HF/6-31G(d) Level^a

| $\text{NgX}^+(\text{state})$ | r_b | ρ_b | $\nabla^2\rho_b$ | H_b | D_e | interactions |
|--------------------------------------|-------|----------|------------------|-------|-------|-----------------|
| $\text{NeLi}^+(\text{X}^1\Sigma^+)$ | 1.206 | 0.10 | 3.57 | 0.06 | 3.0 | electrostatic |
| $\text{NeBe}^+(\text{X}^2\Sigma^+)$ | 1.208 | 0.16 | 4.47 | 0.04 | 0.9 | electrostatic |
| $\text{NeB}^+(\text{X}^1\Sigma^+)$ | 1.249 | 0.10 | 1.45 | 0.01 | 1.2 | electrostatic |
| $\text{NeB}^+(\text{X}^3\Pi)^b$ | 1.167 | 0.30 | 7.32 | -0.10 | 7.3 | covalent |
| $\text{NeC}^+(\text{X}^2\Pi)$ | 1.098 | 0.23 | 3.46 | -0.01 | 3.0 | electrostatic |
| $\text{NeC}^+(\text{X}^1\Sigma^-)^b$ | 1.061 | 0.59 | 12.00 | -0.51 | 21.7 | covalent |
| $\text{NeN}^+(\text{X}^3\Sigma^-)$ | 0.960 | 0.50 | 8.31 | -0.07 | 9.2 | covalent |
| $\text{NeO}^+(\text{X}^4\Sigma^-)$ | 1.168 | 0.14 | 3.19 | 0.04 | 1.2 | electrostatic |
| $\text{NeO}^+(\text{X}^2\Pi)$ | 0.859 | 0.92 | 16.25 | -0.20 | 6.3 | covalent |
| $\text{NeF}^+(\text{X}^3\Pi)$ | 1.022 | 0.30 | 7.50 | 0.07 | 3.6 | electrostatic |
| $\text{NeF}^+(\text{X}^1\Sigma^+)$ | 0.797 | 1.29 | 23.42 | -0.34 | 39.8 | covalent |
| $\text{NeNe}^+(\text{X}^2\Pi)$ | 0.858 | 0.65 | 14.59 | 0.14 | 29.8 | (electrostatic) |
| $\text{ArLi}^+(\text{X}^1\Sigma^+)$ | 1.597 | 0.07 | 1.74 | 0.03 | 5.7 | electrostatic |
| $\text{ArBe}^+(\text{X}^2\Sigma^+)$ | 1.422 | 0.27 | 4.88 | -0.01 | 10.9 | electrostatic |
| $\text{ArB}^+(\text{X}^1\Sigma^+)$ | 1.507 | 0.12 | 1.21 | 0.01 | 5.6 | electrostatic |
| $\text{ArB}^+(\text{X}^3\Pi)$ | 1.321 | 0.61 | 7.39 | -0.41 | 35.2 | covalent |
| $\text{ArC}^+(\text{X}^2\Pi)$ | 1.194 | 0.53 | 2.63 | -0.14 | 20.6 | covalent |
| $\text{ArC}^+(\text{X}^4\Sigma^-)$ | 1.152 | 1.15 | -4.68 | -1.26 | 56.5 | covalent |
| $\text{ArN}^+(\text{X}^3\Sigma^-)$ | 1.050 | 0.98 | 2.13 | -0.49 | 48.7 | covalent |
| $\text{ArO}^+(\text{X}^4\Sigma^-)$ | 1.265 | 0.30 | 5.10 | 0.05 | 10.0 | electrostatic |
| $\text{ArO}^+(\text{X}^2\Pi)$ | 0.911 | 1.53 | -0.83 | -1.08 | 50.5 | covalent |
| $\text{ArF}^+(\text{X}^1\Sigma^+)$ | 0.858 | 1.59 | -0.33 | -1.02 | 43.2 | covalent |
| $\text{ArF}^+(\text{X}^3\Pi)$ | 1.107 | 0.43 | 6.40 | 0.01 | 16.6 | electrostatic |
| $\text{ArNe}^+(\text{X}^2\Pi)$ | 1.257 | 0.15 | 3.25 | 0.02 | 1.8 | electrostatic |

^aThe position r_b is given in Å with respect to the position of the nucleus of Ng. Electron density ρ_b at r_b is given in $\text{e} \text{Å}^{-3}$, Laplacian $\nabla^2\rho_b$ in $\text{e} \text{Å}^{-5}$, energy density H_b in hartree Å^{-3} , and D_e in kcal mol⁻¹. ^bA maximum rather than a saddle point was found.

ρ_b is larger for X = N than for X = O or F. This trend of ρ_b , however, is parallel to the occupation of the frontier orbitals of X^+ .

All ions NeX^+ and ArX^+ investigated in this work fulfill condition a, although in some cases (for example, see NeLi^+ and ArLi^+ in Table IV) the electron density ρ_b at r_b is very low. Furthermore, the energy density H_b is ≥ 0 for all these ions, for which the estimated electrostatic interactions E_{ind} are similar to the calculated dissociation energies D_e (see Table III). The ions are stabilized by charge-induced dipole interactions rather than covalent Ng,X bonding.

A value of $H_b < 0$ is calculated and, hence, covalent bonding is predicted for the ground states of NeN^+ , ArC^+ , ArN^+ , and ArF^+ as well as for all the excited states with the exception of (³ Π) ArF^+ (Table IV). For the ground states, for which E_{ind} can be estimated, predictions are in line with those based on a comparison of D_e with E_{ind} (Table III). There is, however, one exception which indicates that a caveat with regard to these predictions is necessary. For NeNe^+ , $H_b > 0$ is calculated, although a comparison between D_e and E_{ind} suggests covalent bonding. This may be due to an insufficient description of electron and energy density distribution with the basis set used. For example, in the case of $\text{NeC}^+(\text{X}^4\Sigma^-)$ and $\text{NeB}^+(\text{X}^3\Pi)$ spurious maxima rather than a saddle point of $\rho(\mathbf{r})$ are found in the bonding region, also indicating deficiencies of the basis set.

Apart from the exception just mentioned the analysis of $\rho(\mathbf{r})$ and $H(\mathbf{r})$ confirms the results of the frontier orbital model. The concentration holes in the valence shell of X^+ are in the region in which the LUMO is preferentially located (see Figures 4 and 5). The size of the hole is a measure of the acceptor ability of X^+ as is the energy of the LUMO. Both quantities can be used to assess the nature of the interactions between the noble-gas element Ng and the acceptor ion X^+ . This is a general observation which has been made in many cases.²⁷ In this connection it is important to note that the Laplace concentration reflects the effects of all occupied MOs and, therefore, provides a more reliable description than the frontier orbitals.

(26) A referee pointed out that the comparison should be made with electronegativities χ of atomic ions X^+ rather than neutral atoms X. However, $\chi(\text{X}^+)$ shows the same trend for first-row ions as $\chi(\text{X})$: Hinze, J.; Jaffe, H. *J. Phys. Chem.* **1963**, *67*, 1501.

(27) See, for example, the corresponding discussion in ref 3 and in: Cremer, D. In *Theoretical Models of Chemical Bonding*; Springer Verlag: Heidelberg, in press.

We would like to clarify our distinction between covalently bound NgX^+ cations and those ones that are bound by electrostatic interactions. The data for D_e and E_{ind} shown in Table III indicate that the interaction energies caused by electrostatic forces constitute a significant and sometimes dominant part of the total dissociation energy even for NgX^+ cations which are labeled as covalent in our scheme (Table IV). We want to emphasize that our classification is based on a mathematical definition given above which has been shown^{24,25} to be in agreement with the general classification for many molecules. Because covalency is not a physical observable, the definition is arbitrary. Its advantage is that it is uniquely defined^{24,25} and related to the electronic structure at the bond critical point, which is the center of the covalent bond.

Summary, Chemical Relevance, and Outlook

The first-row diatomic cations NeX^+ possess low dissociation energies of < 10 kcal/mol in their electronic ground states. An exception is NeNe^+ , which is stabilized by ca. 30 kcal/mol. The calculated excited states of NeB^+ , NeC^+ , NeO^+ , and NeF^+ are more stable than the respective ground states. These trends are easily explained by invoking donor-acceptor interactions between Ne and X^+ . The magnitude and the trend of these interactions from NeLi^+ to NeNe^+ can be assessed by analyzing frontier orbitals or, more general, the Laplace concentration $-\nabla^2\rho(\mathbf{r})$. An estimate of the electrostatic interaction energies between Ne and X^+ in conjunction with the analysis of the electron density H_b reveals that covalent bonding is likely for X = N and Ne. The ground states of NeLi^+ , NeBe^+ , NeB^+ , NeC^+ , NeO^+ , and NeF^+ are stabilized by charge-induced dipole interactions. Covalent bonding is predicted for all excited states of NeX^+ investigated here.

Similar trends are found for the argon analogues ArX^+ , which are in general more stable than NeX^+ due to the lower ionization energy and higher polarizability of Ar. Covalent bonding in ArX^+ is predicted for X = C, N, F for the ground states and for all excited states except X = F. Some ArX^+ cations are distinguished from the analogues NeX^+ by dissociating into $\text{Ar}^+ + \text{X}$ rather than $\text{Ar} + \text{X}^+$. That is why ArF^+ in the $\text{X}^1\Sigma^+$ ground state possesses a normal electron pair bond rather than a semipolar bond.

The presented theoretical data on the stabilities and electronic structures of light noble gas diatomic ions NgX^+ provide insight into the changes from Ng = He to Ne and Ar, and from X = Li to Ne. The gradual increase in "chemical" character, i.e., covalent

bonding, from helium to neon and argon ions is revealed by the analysis of the electron density distribution. The changes in dissociation energies and binding interactions along the first-row elements X from lithium to neon are not smooth but show a distinct maximum for X = N, which is explained by the electronic structure of X. The analysis of the attractive interactions in NgX⁺ is an important information for the knowledge about chemical bonding, not only for theory but also for experiment. Experimental approaches to synthesize chemically bound neutral compounds of the light noble gases should focus on salts of ArF⁺ and perhaps ArN⁺, which are the most stable NgX⁺ ground-state ions. A recent discussion^{1b} of the chances to isolate argon compounds suggested that AuF₆⁻ and Sb₆⁻ could stabilize ArF⁺ in a salt. Since the stability is critically dependent on the lattice energy of the salt, which in turn depends on the unit volume, the larger ArN⁺ might be less suitable than ArF⁺.

The donor-acceptor model used to explain stabilizing interactions in helium compounds²⁻⁵, NeX⁺ compounds, and ArX⁺ compounds is also used to search for candidates of excimer ion laser sources. The stimulated emission of laser radiation via relaxation of a molecule from a bound excited state (excimer) to an unbound lower lying state, usually the ground state, has been the subject of intensive theoretical and experimental research.²⁸ Many such molecules consist of diatomic species containing noble-gas elements because their ground states are essentially repulsive. However, most investigated systems so far involved neutral molecules.²⁸ Very recently, the feasibility of excimer ions as potential sources of laser radiation at various wavelengths has been proposed in theoretical papers by Sauerbrey and Langhoff²⁹ and Basov et al.³⁰ Even doubly charged cations such as the noble-gas

halide dications have been discussed by Jonathan et al.³¹ as potential laser sources. Ionic systems are very interesting because the laser wavelength may be shorter than what is possible for neutral molecules.³⁰ Also, the ground states of NgX⁺ molecules are more strongly bound than neutral NgX molecules because of the charge-induced dipole interactions. This may yield higher transition probabilities although a too strongly bound ground state will prohibit the release of laser radiation.

Theoretical studies of cations can be helpful for experimentalists searching for promising molecules as sources of laser radiation. Accurate ab initio calculations may predict the transition probability of a particular system and the laser wavelength. However, a systematic search for potential laser systems necessitates a model that helps in understanding the underlying bonding features of the molecules. Such an understanding is provided by the donor-acceptor model discussed here. Our study can help to select promising ionic species by allowing a priori estimates of the possible bound states of diatomic NgX⁺ species. Further theoretical studies require high-level ab initio calculations of the potential energy surfaces of the candidate molecules. Work on this is in progress.

Acknowledgment. We acknowledge stimulating discussions on noble-gas chemistry with Prof. Neil Bartlett. Excellent service and necessary computer time at the CRAY-XMP/48 was provided by a grant from the San Diego Supercomputer Center. D.C. thanks the Deutsche Forschungsgemeinschaft and the Fonds der Chemischen Industrie for financial support.

Registry No. Ne, 7440-01-9; Ar, 7440-37-1; Li⁺, 17341-24-1; Be⁺, 14701-08-7; B⁺, 14594-80-0; C⁺, 14067-05-1; N⁺, 14158-23-7; O⁺, 14581-93-2; F⁺, 14701-13-4; Ne⁺, 14782-23-1; Ar⁺, 14791-69-6.

(28) Rhodes, C. K. (Ed.) *Excimer Lasers*; Springer Verlag: Berlin, 1979.
(29) Sauerbrey, R.; Langhoff, H. *IEEE J. Quantum Electron.* **1985**, QE-21, 179.

(30) (a) Basov, M. G.; Voltik, M. G.; Zuev, V. S.; Kutakhov, V. P. *Sov. J. Quantum Electron.* **1985**, 15, 1455, 1461.

(31) Jonathan, P.; Brenton, A. G.; Beynon, J. H.; Boyd, R. K. *Int. J. Mass Spectrom. Ion Processes* **1987**, 76, 319.

(32) Moore, C. E. *Atomic Energy Levels*; National Bureau of Standards; U.S. Government Printing Office: Washington, DC, 1971; NSRDS-NBS 35.

Mass Spectrometric Study of Negative Ions from Acetyl Derivatives

J. Hacaloglu, A. Gokmen, and S. Suzer*

*Department of Chemistry, Middle East Technical University, 06531 Ankara, Turkey
(Received: February 26, 1988; In Final Form: November 17, 1988)*

A mass spectrometric technique capable of producing a low-energy and nearly monochromatic (fwhm ~ 0.2 eV) electron beam is developed and used to study the negative ions from five different acetyl derivatives CH₃COX (X = Cl, C₆H₅, NH₂, CH₃, and H) at very low energies (0-10 eV). Negative ions are mainly produced by dissociative attachment and show resonance-like structures. To measure the excess energy imparted to the ions during ionization, a time-of-flight technique is applied. An ion with composition C₂H₃O⁻ is the common ion, and its appearance potential is different from different molecules. With use of the available data on bond energies and the excess energy equated to zero, electron affinity of the corresponding radical, C₂H₃CO, can be calculated; this varies between 2.3 and 2.7 eV for these five molecules. This value is rather high compared with the known electron affinity of CH₃CO, 0.42 eV, measured by the technique of flowing afterglow, and is much closer to 1.817 eV, the reported electron affinity of its structural isomer, the enolate radical, CH₂=CH-O. Therefore, isomerization during or after dissociation of the parent ion is suggested as a possibility.

Introduction

Although the interest in negative ionization processes has increased in recent years, the knowledge is incomplete from purely physical aspects (i.e., determination of appearance potentials, electron affinities, or electron-capture cross sections, etc.).^{1,2} The electron attachment processes of acetyl derivatives at normal mass spectrometric conditions (low pressure, 70 eV) and at increased

source pressure (ca. 1 mbar) have been the subject of many experimental studies.³⁻⁵ Also, they have been investigated by the technique of flowing afterglow. However, not much is known about negative ionization processes of these compounds with very low energy electrons.

In this work, we report a mass spectrometric study of negative ionization processes of some acetyl compounds CH₃COX where

(1) Dillard, J. G. *Chem. Rev.* **1973**, 73, 589.
(2) McCorkle, D. L.; Christophoulides, A. A.; Christophorou, L. G.; Szamrej, I. *J. Chem. Phys.* **1980**, 72, 4049.

(3) Budzikiewicz, H. *Angew. Chem., Int. Ed. Engl.* **1981**, 20, 624.
(4) Aplin, R. T.; Budzikiewicz, H.; Djerassi, C. *J. Am. Chem. Soc.* **1965**, 87, 3180.
(5) DeSouze, B. C.; Green, J. M. *J. Chem. Phys.* **1967**, 46, 1421.